

The Structure and Activity of Supported Metal Catalysts

III. Desorption of Carbon Monoxide-¹⁴C from Platinum/Silica Impregnated Catalysts

D. CORMACK AND R. L. MOSS

From the Warren Spring Laboratory, Stevenage, England

Received May 30, 1968; revised September 10, 1968

The desorption of carbon monoxide labeled with carbon-14 from Pt/silica catalysts was followed with a Geiger-Müller tube mounted directly over the catalyst sample. Varying amounts of CO could readily be desorbed depending on the Pt content of the catalyst; the remainder was more strongly adsorbed. Platinum crystallite size distributions were determined from X-ray line-broadening, the proportion of Pt detectable by X-ray diffraction, and electron micrographs of ultramicrotome sections. The percentage of readily desorbed CO was greatest on small crystallites occurring in catalysts with low Pt content.

By comparison with previous infrared work, the two types of CO identified from these desorption studies are correlated with linear and bridged species, the latter being more strongly bonded. Present quantitative measurements of the relative amounts of each type make it possible to calculate the number of exposed Pt atoms from CO adsorption results.

The variation of the relative numbers of linear and bridged CO molecules is explained in terms of the fractions of the platinum surface composed of edge and plane atoms (with low and high coordination numbers). The necessary crystallite-size variation of these fractions is found by considering the crystallites to be perfect cubo-octahedra exposing (100) and (111) faces with additional incomplete layers of Pt atoms on the faces placed either randomly or as close-packed islands. Comparisons are made between these models and experimental results.

INTRODUCTION

While the metal area in supported catalysts can be estimated from crystallite-size measurements using X-ray line-broadening, electron microscopy, and other physical methods (1-3), CO chemisorption is commonly used (4, 5) as a direct quantitative method. The basis of the method is the existence of conditions where CO will chemisorb selectively on the metal but not on the support and a knowledge of the ratio (metal atoms exposed)/(CO molecules adsorbed).

However, the infrared spectra of CO adsorbed on supported palladium, platinum, nickel (6), and rhodium (7) show two distinct absorption bands. By analogy with the spectra of the metal carbonyls, the high-frequency band has been ascribed to a linear* surface species in which the carbon atom of the adsorbed CO molecule is bonded to one surface metal atom, and the low-frequency

band to a bridged species in which the carbon atom is bonded to two metal atoms (8). Furthermore, the relative intensities of these bands vary with metal content (9) and nature of support material (10). Because no reliable extinction coefficients are available (10) the band intensities corresponding to the two types of bonding cannot be translated into surface coverages. Therefore the relative amounts of carbon monoxide adsorbed in the linear and bridged forms are unknown and there is considerable uncertainty in determining the number of surface metal atoms from the amount of carbon monoxide adsorbed.

An attempt is made to overcome this

* The terms 'linear' and 'bridge' bonded carbon monoxide, originating from previous infra-red studies, are used throughout to denote adsorption which gives (Pt exposed)/(CO adsorbed) ratios of 1 and 2 respectively.

difficulty in the following way: The high-frequency infrared absorption band is always removed first on evacuation whereas the low-frequency band is removed more slowly (8). Thus it might be possible to relate the amounts of carbon monoxide desorbed under certain conditions with the fractions of the metal surface covered by each type of chemisorbed carbon monoxide molecule. Therefore the desorption of carbon monoxide-¹⁴C was studied using the *in situ* radiotracer system previously described (11). The procedure requires the direct monitoring of surfaces by means of a Geiger-Müller tube. Fractional coverages can be determined by relating a given count rate to that observed for a complete monolayer. Rates of desorption of carbon-14-labeled carbon monoxide can be examined and the coverage remaining when weakly bonded carbon monoxide has been desorbed, can be measured. Hence it might be possible to obtain quantitative information about the extent to which the two types of bonding occur.

The suggestion that the relative amounts of the two types vary with the weight percent of metal present was also investigated. A series of Pt/silica catalysts with increasing Pt content was used and characterized by X-ray diffraction and electron microscopy. From this information on platinum crystallite-size distribution, the nature of the sites involved in different types of bonding can be discussed.

APPARATUS AND MATERIALS

The adsorption vessel incorporating a Geiger-Müller tube for monitoring the uptake of carbon-14-labeled compounds on the catalyst surface has already been described (11). The catalysts were caused to adhere to a glass holder by slurring with montmorillonite and drying at 100°C (12). The catalyst sample (10 mg) was placed in a 1.3-cm diameter depression in the holder in such a way that the top surface of the sample was level with the surrounding flat glass surface of the holder. After reducing the catalyst in a stream of hydrogen the holder could be moved by an external magnet to the Geiger-Müller tube region. With such a system counts may be taken of surface

plus gas-phase activity. The gas-phase contribution alone may then be obtained by taking counts over the glass plate to one side of the catalyst sample. In this position the Geiger-Müller tube is exposed to the same gas volume as before and the surface count may be obtained by difference. The geometry of the system was strictly reproducible for a given specimen of catalyst since undesirable movement of the holder was prevented by a PTFE (polytetrafluoroethylene) guide.

The catalysts were prepared by impregnating Davison grade 70 silica gel with solutions of chloroplatinic acid. The water was boiled off and the solid dried at 120°C for 16 hr in an air oven. Four catalysts were prepared containing, respectively, 8.8, 3.0, 1.24, and 0.14 wt % platinum. These catalysts were given an initial 2-hr reduction in a stream of hydrogen at 210°C. A fifth catalyst containing 10.1% was heated in hydrogen at 500°C for 2 hr (designated 10.1% Pt/500R). Before each experiment the catalysts were reduced *in situ* at 210°C for 2 hr in a 50 ml/min hydrogen stream followed by evacuation for 16 hr at the same temperature.

In the gas-handling system greaseless stopcocks were used with Viton A diaphragms for gas control. Pressures were measured in the range 1-50 torr with a pressure transducer of the strain gauge type and below 1 torr they were monitored by a combined Pirani-Ionisation gauge. Breakseal glass ampoules of ¹⁴CO (specific activity 50 mCi/mmole) were glass-blown to the system and the gas was diluted where necessary with nonactive "spectroscopically pure" carbon monoxide (British Oxygen Co., Ltd.).

EXPERIMENTAL PROCEDURE AND RESULTS

The desorption of ¹⁴CO was studied in two cases, viz., where equilibrium gas pressure over the catalyst prior to the start of desorption measurements was either 4-5 torr (referred to subsequently as a high-pressure experiment) or 0.1 torr (a low-pressure experiment).

For the high-pressure experiments it was necessary to dilute the original ¹⁴CO with

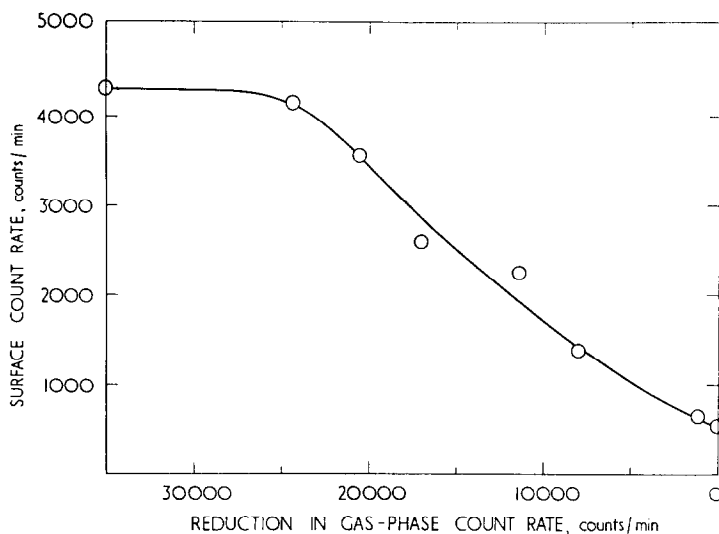


FIG. 1. Desorption by successive expansions of labeled CO from a 1.24% Pt/silica catalyst saturated at 4-5 torr.

nonlabeled carbon monoxide by a factor of approximately 50. For the low-pressure work the ^{14}CO was used as supplied and this enabled satisfactory counting statistics to be obtained at the low coverages involved. In both types of experiment labeled gas was admitted to the predetermined equilibrium pressure. Desorption was carried out by successive expansions into an evacuated volume to reduce the gas pressure over the catalyst. Finally the system was directly connected to the pumps.

For the high-pressure experiments it was found that initially the surface maintained its count rate as the pressure was reduced by expansion, showing that it had been saturated at a pressure of 4-5 torr. With further pressure reduction by expansion, desorption commenced and continued until the gas-phase count rate reached the background value. A typical desorption curve down to a gas-phase count of background level is shown in Fig. 1. At this point not all the initially adsorbed carbon monoxide had been desorbed and the remainder could be removed only slowly by pumping. The percentage of the total adsorbed carbon monoxide which desorbs easily on expansion is shown in Table 1, for each catalyst. It would appear that the amount of easily desorbed carbon monoxide varies from one catalyst

sample to another. It should be pointed out that the observed activities can only be used to determine relative amounts of carbon monoxide present. Because the extent of self-absorption of the β -particles in the catalyst samples was not determined, activities cannot be converted to actual numbers of moles even if the specific activity was accurately known.

If it is assumed that the strongly held carbon monoxide (slowly desorbed by prolonged pumping) was adsorbed first, then at low coverages it should represent a greater proportion of the adsorbed molecules. Hence desorption from partially covered surfaces (equilibrium pressure 0.1 torr) was measured and the results are summarized in Table 1. These low-pressure results confirm the trend in the amounts of carbon monoxide desorbed

TABLE 1
 ^{14}CO DESORPTION FROM Pt/SILICA CATALYSTS

Pt content (%)	% ^{14}CO desorbed Pressure before desorption—		θ_{obs}	θ_{calc}
	0.1 torr	4-5 torr		
0.14	53.5	93	0.10	0.15
1.24	31.0	87	0.13	0.18
3.0	11.0	85	0.18	0.17
8.8	6.0	72	0.32	0.30
10.1/500R	3.5	56	0.48	0.45

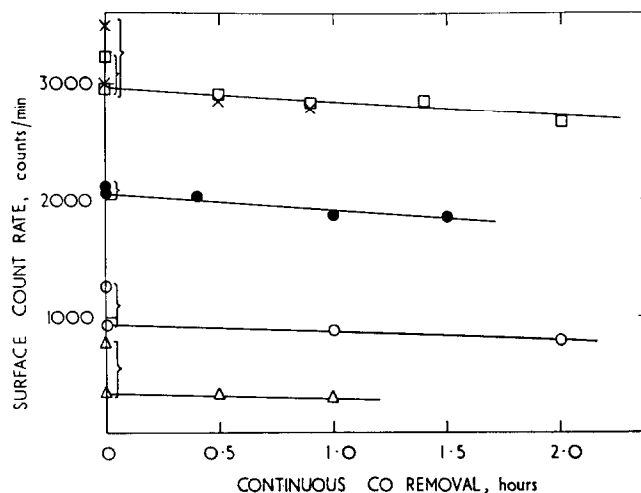


FIG. 2. Desorption by continuous pumping of labeled CO from silica-supported catalysts containing, Δ , 0.14% Pt; \circ , 1.24% Pt; \times , 3% Pt; \square , 8.8% Pt; and \bullet , 10.1% Pt. Brackets show amount of CO removed by expansion before continuous pumping.

and, as expected, the percentage desorbed is less than that observed when starting from saturation coverage.

Because carbon monoxide of high specific activity could be used and the counting rate increased in these experiments, the desorption with time of the usually small amount of strongly bonded carbon monoxide could be studied more accurately. Plots of the desorption rate under pumping conditions are shown in Fig. 2. These plots show the clear distinction which can be made between weak and strong bonding on the basis of desorption rate. Further, the similarity in gradient indicates that the same two types of bonding occur on each catalyst.

It also seemed important to test the internal consistency of results at high and low coverages in the following way: Suppose that the fraction of the surface covered by strongly bonded molecules is θ_s (measured in the high-pressure experiments) so that the number of strongly held molecules is $N\theta_s$ where N is the total number of adsorbed molecules. Let θ_{calc} be the fraction of the surface covered at 0.1 torr and which is to be computed. Then if x is the fractional coverage of strongly held CO at 0.1 torr, the number of strongly held molecules at this equilibrium pressure is $xN\theta_{\text{calc}}$. Since $N\theta_s$ is equivalent to $xN\theta_{\text{calc}}$, θ_{calc} can be determined and the values are

presented in Table 1. Coverages at 0.1 torr were observed in the course of the high-pressure experiments and these are also presented in Table 1 under the heading θ_{obs} . The agreement in the values indicates satisfactory correlation between the high- and low-pressure experiments, confirming the assumption that the two types of surface species adsorb in the reverse order of their desorption.

Thus two distinct types of adsorption of carbon monoxide on Pt/silica catalysts have been demonstrated on the basis of strength of bonding. It is further apparent that the weak bonding mode decreases in extent as the weight percent of metal increases.

Information on the platinum crystallite size in all the samples studied is presented in the next section.

Crystallite Size

An understanding of the platinum size distribution was built up by a combination of X-ray line-broadening measurements and examination of electron micrographs of ultramicrotome sections.

Measurements of mean crystallite size by X-ray line-broadening in this series of catalysts are recorded in Table 2 together with the fraction of total platinum detected by X-ray diffraction, i.e., crystallites of 50 Å

TABLE 2
CRYSTALLITE SIZE

Pt content (%)	Pt detected by X-ray diffraction		Pt detected by electron microscopy		Area in crystallites <50 Å (%)
	Crystallite size (Å)	Fraction of total Pt detected	Mean size <50 Å	Mean size >50 Å	
0.14	No diffraction lines observed		27	—	~100
1.24	70	0.43	29	55	79
3.0	60	0.44	25	63	75
8.8	90	0.88	25	76	33
10.1/500R	105	0.95	22	99	18

and above. The amount of platinum present in the highly dispersed form, less than 50-Å diameter and not included in the determination, was estimated as follows (13): The area under the diffraction line profile was measured relative to a catalyst where all the platinum had been grown to a detectable crystallite size by firing in air at 800°C before reduction. Total platinum content in all cases was measured by X-ray fluorescence analysis and hence the amount of platinum in the highly dispersed form could be calculated.

Platinum could not be detected by X-ray diffraction in the catalyst containing 0.14% Pt which is therefore the most highly dispersed in the series. It is clear from columns 2 and 3 that crystallite size increased with platinum content.

However, the prime concern in the present work is the area available for carbon monoxide chemisorption deriving from crystallites of various sizes. The data in columns 2 and 3 were used to calculate the area due to crystallites above and below 50 Å. The metal area of an amount of catalyst containing 1 g of platinum is given by $5 \times 10^4 / l\rho$, where l is the edge length of the cube in angstrom units and ρ is the density of platinum. Hence the percentage of the total area due to crystallites <50 Å was found (column 6). In calculating the area of the crystallites <50 Å, a mean value of 25 Å derived from electron microscopy was used (see below).

Electron micrographs (Fig. 3), showed that the platinum was evenly distributed as crystallites of varying size throughout the pore structure of the silica gel. At least 1000 crystallites in each micrograph were sized in terms of their diameters in 10 Å increments (Fig. 4).

The volume weighted mean diameter d_v was derived for crystallites above and below 50 Å from,

$$d_v = \Sigma N_i d_i^4 / \Sigma N_i d_i^3$$

where there are N_i crystallites of diameter d_i . If the crystallites are spherical, these sizes can be compared with sizes derived from X-ray data which are taken as the cube root of the crystallite volume, V , implying an isodimensional model, thus

$$V^{1/3} = (\pi/6)^{1/3} d_v = 0.806 d_v$$

Values of 0.806 d_v are recorded in Table 2 for crystallites above and below 50 Å size (columns 4 and 5). From the number of crystallites N_i of diameter d_i the percentage of the total area due to crystallites of each size was calculated,

$$\% \text{ area} = (N_i d_i^2 / \Sigma N_i d_i^2) \times 100$$

Figure 5 shows this information for some of the catalysts used in the present work.

With increased platinum content, a greater proportion of the area is due to the larger crystallites. While Fig. 5 illustrates this trend clearly, % areas derived from X-ray data were used since the electron micrograph sample is extremely small. Furthermore, the % area is very sensitive to the number of larger crystallites observed in the electron micrograph. However, a great many small crystallites can be sized and counted in each sample (see Fig. 4) and these should give a reasonably accurate estimate of the mean size of crystallites <50 Å in diameter.

DISCUSSION

The results show clearly that the relative amount of weakly held carbon monoxide decreases as the crystallite size of the plati-

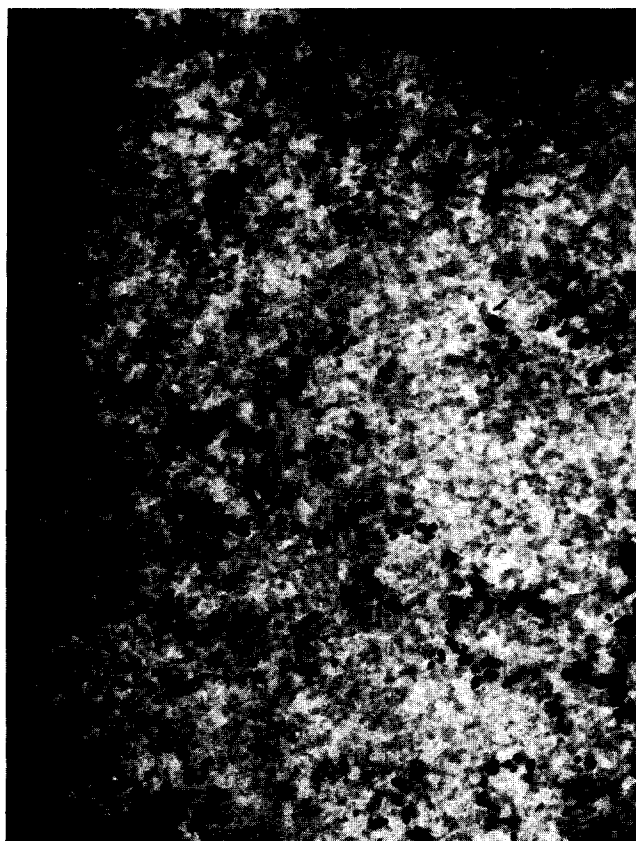


Fig. 3. Electron micrograph from ultramicrotome section of a 10.1% Pt/silica catalyst reduced at 500°C. Magnification: 100 000 \times .

num increases. The distinction between weakly and strongly bonded carbon monoxide was made by the rates of desorption as was done in previous infrared studies with supported palladium and nickel catalysts (8, 9). Therefore the present work confirms the infrared observations that nickel (9) and palladium (14) crystallite size affects the strength of the carbon monoxide bonding. This agreement supports the assumption that both the infrared and tracer techniques are dealing with the same adsorbed carbon monoxide species. Assuming platinum to behave as nickel and palladium, the radio-tracer approach therefore enables measurement to be made of the extent to which each type occurs on supported metal catalysts. Furthermore, if the assignment of linear and bridge bonding to the weakly and strongly bonded carbon monoxide is correct it becomes possible to determine the number of platinum atoms exposed.

However, it has recently been suggested that bridge bonding does not occur and that the infrared absorption bands correspond to different strengths of linear bonding (15), the strong bonding occurring on low co-ordination number atoms as a result of less competition from neighboring metal atoms for the available metallic bonding electrons. Thus strongly bonded carbon monoxide would be expected on edge and corner atoms. Now consideration of model crystallites (cubo-octahedra) indicates that surface topography changes as the size of the crystallites increase (16). In particular, the number of surface atoms of low coordination number (at edges and corners) decreases with respect to those on extended planes showing high coordination numbers. Thus it would follow that as crystallite size is increased, less strongly bonded carbon monoxide should be observed. This expectation is contrary both to the present results and the infrared obser-

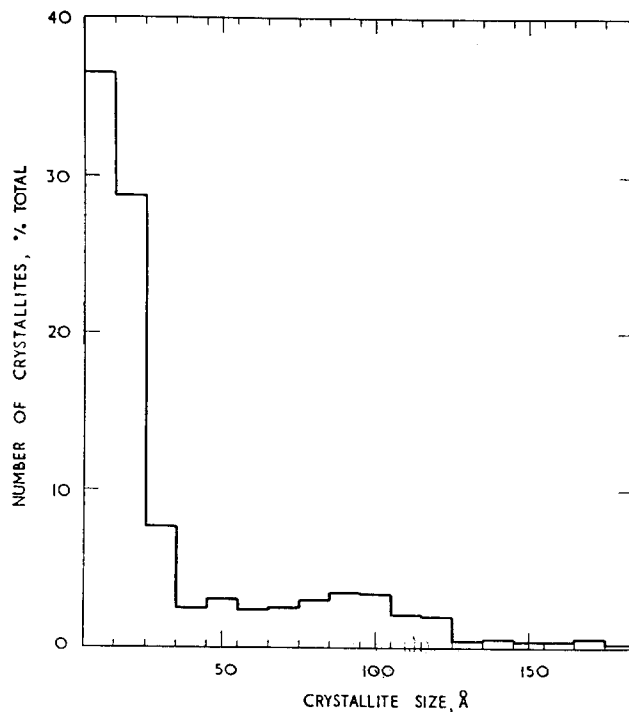


Fig. 4. Size distribution of platinum crystallites in 10.1% Pt/silica catalyst, derived from Fig. 3

vations on supported nickel and palladium catalysts (9, 14).

Because knowledge of the crystallite-size distribution is crucial to this discussion, both X-ray diffraction and electron microscopy were used to characterize the catalysts used in the present work. At the lowest

platinum content this series of platinum/silica catalysts had $\sim 100\%$ of total area due to crystallites $< 50 \text{ \AA}$. At the highest platinum content only 18% of the total area was due to crystallites of this size.

However, a synthesis of these apparently opposing views may be arrived at by sup-

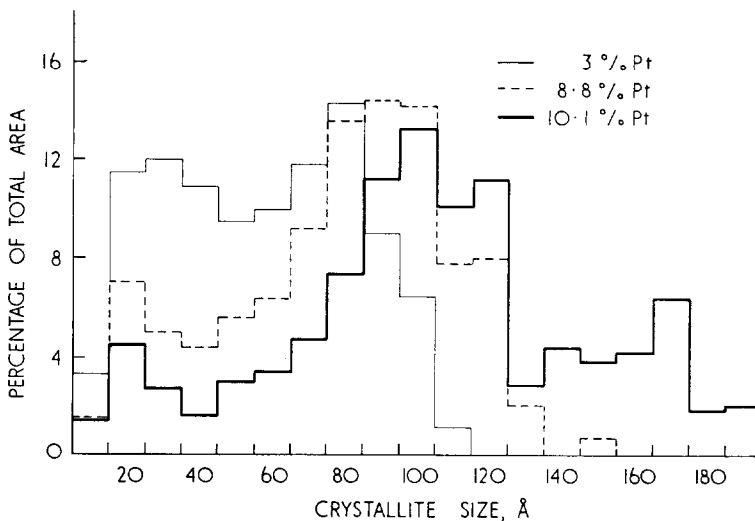


Fig. 5. Percent of total area due to crystallites of various sizes observed in electron micrographs of catalysts containing 3%, 8.8%, and 10.1% Pt supported on silica.

posing that linear bonding is indeed stronger on edges than on planes for the reasons given, but that on planes, because of neighboring metal atoms, it is superceded by bridge bonding which results in even more strongly held species.

The percentages of easily desorbed carbon monoxide observed in this work are discussed below in quantitative terms on the assumption that linearly bonded carbon monoxide is present on edge atoms (Pt/CO ratio = 1) and bridge-bonded carbon monoxide on extended planes (Pt/CO ratio = 2).

For reasons which will emerge later the crystallite-size distribution is effectively described by the fractions of the total area in sizes $<50 \text{ \AA}$ or $>50 \text{ \AA}$ determined by X-ray diffraction (Table 2, column 6). If the areas arising from crystallites $<50 \text{ \AA}$ and $>50 \text{ \AA}$ are A_s and A_1 , respectively, and the fractions of these areas composed of edge atoms are f_s and f_1 then the fraction of carbon monoxide desorbed (linearly bonded) is given by,

Fraction Desorbed

$$= \frac{2(f_s A_s + f_1 A_1)}{A_s(1 + f_s) + A_1(1 + f_1)}$$

Since the catalyst containing 0.14% Pt

contains effectively no crystallites $>50 \text{ \AA}$, $f_1 A_1 = 0$ in this case and hence $f_s = 0.87$. Using $f_s = 0.87$ and observed fractions of easily desorbed CO, values of f_1 were calculated for all the other catalysts, yielding a mean value of $f_1 = 0.35$. Values of the carbon monoxide fraction desorbed, calculated using $f_s = 0.87$ and $f_1 = 0.35$, are recorded in Table 3 and show the agreement

TABLE 3
 ^{14}CO DESORPTION CALCULATED FROM FRACTION
EDGE SITES, f ON CRYSTALLITE SURFACE

Pt content (%)	% ^{14}CO desorbed (initially full coverage)	
	Observed	Calculated ($f_s = 0.87$; $f_1 = 0.35$)
0.14	93	93
1.24	87	86
3.0	85	86
8.8	72	68
10.1/500R	56	61

with the observed values. It seems significant that although A_1 shows a large variation through the series, nevertheless, a constant value of f_1 provides good agreement between calculated and observed fractions of carbon monoxide desorbed. It would appear that the

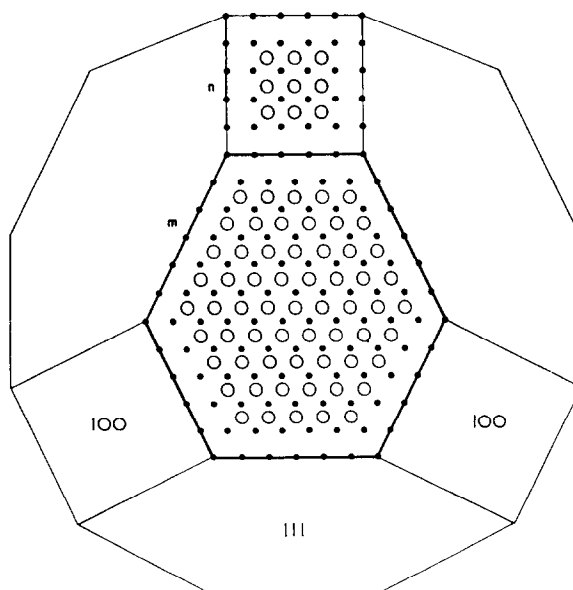


FIG. 6. View of cubooctahedral crystallite showing atoms on adjacent (100) and (111) faces, ●; and additional atoms, ○ on these faces.

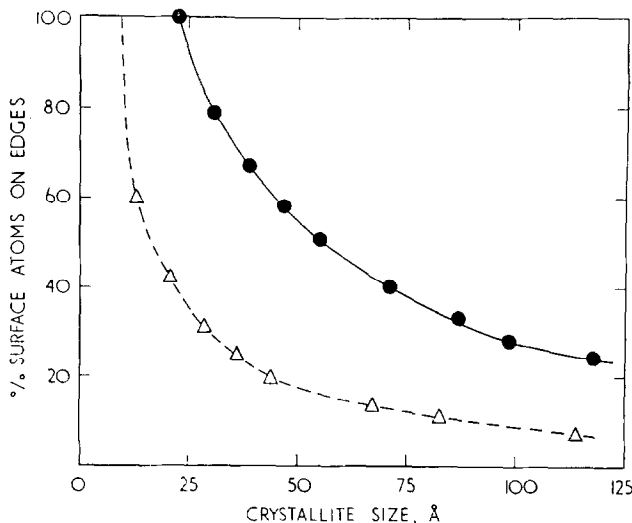


FIG. 7. Number of edge atoms on perfect cubooctahedral crystallites of varying size, --Δ--, and on crystallites with complete ad-layers corresponding to Fig. 6, —●—.

assignment of linear and bridged carbon monoxide to edge and plane adsorption sites as described above is a reasonable assumption.

In the following section a model is developed which provides relative numbers of edge and plane sites as a function of crystallite size. The assumptions involved are as follows.

The crystallites are cubooctahedra which expose preferentially the (111) and (100) planes, i.e., approximating closely to spheres and exposing highly coordinated planes (16). Figure 6 shows adjacent cubic and octahedral planes where $m = 7$ and $n = m - 1$. It was found in the present work that crystallite sizes derived from (111), (200), (311), etc., X-ray lines are approximately the same using a fixed value of the Scherrer constant. Although a constant value, strictly speaking, only applies to spheres, it is nearly correct for cubes, octahedra, etc. Platelets or other extreme shapes would give rise to varying values of crystallite size calculated from different X-ray lines.

Figure 7 shows the number of edge atoms on perfect cubooctahedra $n = m - 1$ (compare Fig. 6) as a fraction of the total number of surface atoms (broken line) for crystallites of varying size, d_{sph} , given by

$$d_{\text{sph}} = 1.11(N_{\text{total}})^{1/3} \times 2.77$$

where N_{total} is the number of atoms in the crystallite (16). While this curve shows the required trend of decreasing numbers of edge atoms (linear bonding sites) nevertheless actual f values are too low. Perfect cubooctahedra, however, only occur when certain fixed numbers of atoms are present.

Because the catalysts are prepared by impregnation there will be a random number of atoms in each crystallite resulting in additional incomplete layers on the various faces of the underlying perfect crystallites. These extra atoms create more edge sites for linear bonding. It would appear that there are two ways of adding these extra atoms to the perfect cubooctahedra which might profitably be considered. These are random addition of single atoms or the buildup of a close-packed island of atoms.

Figure 8 shows the result (broken line) of adding atoms to the perfect cubooctahedron for a small (30 Å) and a large (85 Å) crystallite using tables of random numbers. Initially, as atoms are added randomly, sites for linear bonding are created and sites for bridge bonding on the underlying perfect cubooctahedron are destroyed. It is assumed that isolated atoms on an edge are not available for bridge bonding. Eventually, however, the randomly added atoms begin to form small islands and thus sites for bridge bonding

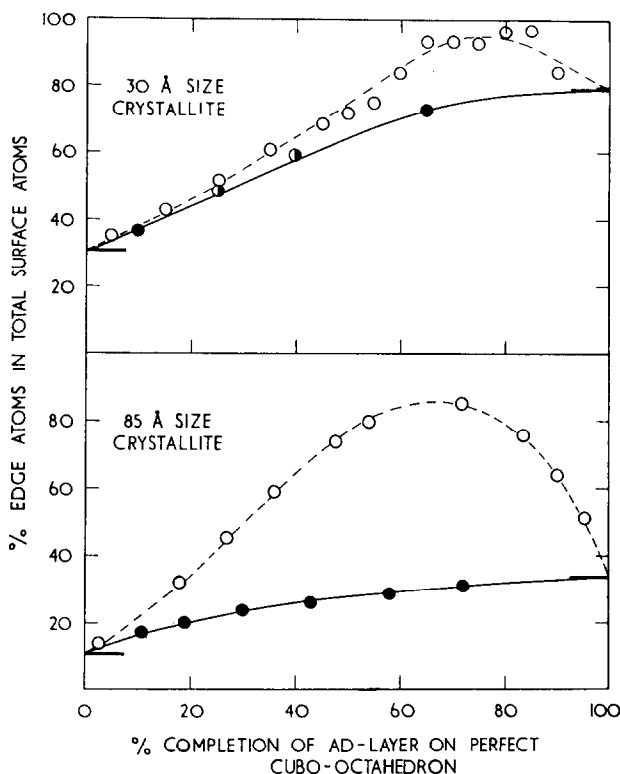


FIG. 8. Number of edge atoms on perfect cubooctahedral crystallites on which adatoms have been placed randomly, --○--; adatoms form close-packed expanding islands, ●, and also have shape of underlying face, ●. Short horizontal bars at 0% and 100% completion correspond to positions on the lower and upper curves of Fig. 7.

are again created. Hence, the maximum observed in the broken line curves of Fig. 8.

The 100% completion of the randomly formed "ad-layer" represented in Fig. 6 corresponds to the maximum B₆-site situation in the van Hardeveld and van Montfoort treatment (16). In both cases small areas of (110) and (113) planes are produced. However, below ~ 20 Å, these planes are not formed, whereas in the present case edge atoms continue to be present down to the very smallest sizes.

The solid line curves in Fig. 8 show, for the same two crystallite sizes (30 and 85 Å), the effect of building up the ad-layer as an expanding close-packed island having the same shape as the underlying face. Of course, the island eventually reaches the 100% completion encountered in the random case.

Inspection of the curves for additions to 30 and 85 Å size crystallites (broken lines,

Fig. 8) indicates that little crystallite size effect on the mode of carbon monoxide desorption would be expected if random addition was the rule. On the not unreasonable assumption that on average the crystallites will have approximately 50% completion of the ad-layer, both random curves yield values of approximately 75% edge atoms. The effect of crystallite size on the desorption of carbon monoxide observed in this work indicates that close-packed addition is more likely.

However, some random addition might be expected, thus increasing the percent edges derived from the mean position on the "regular" curve (solid line Fig. 8). Therefore it is believed that the percent edges calculated at 100% completion might approximate to the real situation. Accordingly the fraction of edge atoms at 100% completion, corresponding to the situation shown in

Fig. 6, was calculated for a number of crystallite sizes, d_{sph} , again using the above equation where N_{total} is now the sum of the atoms in the basic cubooctahedron plus those in the ad-layer.

The addition of a complete layer to other cubo-octahedra based on $n = m$ and $n = m + 1$ for various values of m , provides further points lying on the curve shown in Fig. 7.

The following comparison with the experimental results is now made. The mean size of the crystallites less than 50 Å was seen in electron micrographs to be ~ 25 Å. The value of f_{25} (i.e., the fraction of edge atoms in the total surface of a 25-Å size crystallite) obtained from the curve for 100% completion of the ad-layer (Fig. 7, solid line) is 0.92, in close agreement with 0.87 found experimentally for f_e . For the larger crystallites the fractions of edge atoms in the total surface obtained from Fig. 7, f_{60} , f_{70} , f_{90} , and f_{105} give a mean value of 0.37 compared with the experimental value of $f_1 = 0.35$.

In summary, the present results demonstrate the existence of two types of carbon monoxide bonding on the basis of ease of desorption. The proportion of weakly bonded carbon monoxide decreases with increasing crystallite size. Further, the experiment results can be interpreted in terms of the relative numbers of edge atoms on perfect cubooctahedral crystallites with the extra

atoms, which must be present, disposed as predominantly close-packed ad-layers.

REFERENCES

1. SCHOLTEN, J. J. F., AND VAN MONTFOORT, A., *J. Catalysis* **1**, 85 (1962).
2. ADAMS, C. R., BENESI, H. A., CURTIS, R. M., AND MEISENHEIMER, R. G., *J. Catalysis* **1**, 336 (1962).
3. DORLING, T. A., AND MOSS, R. L. *J. Catalysis* **7**, 378 (1967).
4. GRUBER, H. L., *J. Phys. Chem.* **66**, 8 (1962).
5. HUGHES, T. R., HOUSTON, R. J., AND SIEG, R. P. *Ind. Eng. Chem. Proc. Design Develop.* **1**, 96 (1962).
6. EISCHENS, R. P., FRANCIS, S. A., AND PLISKIN, W. A., *J. Phys. Chem.* **60**, 194 (1956).
7. YANG, A. C., AND GARLAND, C. W., *J. Phys. Chem.* **61**, 1504 (1957).
8. EISCHENS, R. P., AND PLISKIN, W. A., *Advan. Catalysis* **10**, 1 (1958).
9. YATES, J. T., AND GARLAND, C. W., *J. Phys. Chem.* **65**, 617 (1961).
10. O'NEILL, C. E., AND YATES, D. J. C., *J. Phys. Chem.* **65**, 901 (1961).
11. CORMACK, D., THOMSON, S. J., AND WEBB, G., *J. Catalysis* **5**, 224 (1966).
12. SCHUIT, G. C. A., AND VAN REIJEN, L. L., *Advan. Catalysis* **10**, 242 (1958).
13. DORLING, T. A., AND MOSS, R. L., *J. Catalysis* **5**, 111 (1966).
14. CLARKE, J. K. A., FARREN, G., AND RUBALCAVA, H. E., *J. Phys. Chem.* **71**, 2376 (1967).
15. BLYHOLDER, G., *J. Phys. Chem.* **68**, 2772 (1964).
16. VAN HARDEVELD, R., AND VAN MONTFOORT, A., *Surface Sci.* **4**, 396 (1966).